Plant Physiol. (1997) 115: 1515–1524

Visualization of Freezing Behaviors in Leaf and Flower Buds of Full-Moon Maple by Nuclear Magnetic Resonance Microscopy

Masaya Ishikawa*, William S. Price, Hiroyuki Ide, and Yoji Arata

Department of Genetic Resources, National Institute of Agrobiological Resources, Kannondai, Tsukuba, Ibaraki 305, Japan (M.I.); and Water Research Institute, Sengen 2–1–6, Tsukuba, Ibaraki 305, Japan (W.S.P., H.I., Y.A.)

^{1}H-Nuclear magnetic resonance (NMR) microscopy was used to study the freezing behavior of wintering buds of full-moon maple (*Acer japonicum* Thunb.). The images obtained predominantly reflected the density of mobile (i.e. non-ice) protons from unfrozen water. A comparison of NMR images taken at different subfreezing temperatures revealed which tissues produced high- and low-temperature exotherms in differential thermal analyses. In leaf and flower buds of *A. japonicum*, the scales and stem bark tissues were already frozen by −7°C, but the primordial inflorescence and terminal primordial shoots remained supercooled at −14°C, and the lateral primordial shoots were unfrozen even at −21°C. The freezing of these supercooled tissues was associated with their loss of viability. The size of the supercooled primordial shoots and inflorescences was gradually reduced with decreasing temperature, indicating extraorgan freezing in these tissues. During this process the formation of dark regions beneath the primordia and subsequent gradual darkening in the basal part of supercooled primordia were visible. As the lateral shoot primordia were cooled, the unfrozen area was considerably reduced. Since the lateral primordia remained viable down to −40°C, with no detectable low-temperature exotherms, they probably underwent type I extraorgan freezing. Deep supercooling in the xylem was clearly imaged. NMR microscopy is a powerful tool for noninvasively visualizing harmonized freezing behaviors in complex plant organs.

Wintering tissues of temperate woody plant species are known to display diverse freezing behaviors such as extracellular freezing (e.g. bark), deep supercooling (e.g. xylem ray parenchyma), and extraorgan freezing (e.g. flower buds and leaf buds) (Sakai and Larcher, 1987) under subfreezing temperatures. These freezing behaviors are species and tissue specific and are important determinants of cold-hardiness. Freezing behaviors in the xylem of temperate woody species have been studied rather extensively in relation to their geographical and phylogenic distribution (George et al., 1974; Kaku and Iwaya, 1979; Becwar et al., 1981). In contrast, freezing behaviors of winter buds have been studied in a narrow spectrum of species such as *Rhododendron*, *Prunus*, *Rubus*, and conifers (Quamme, 1995). Leaf and flower buds are important organs for the vegetative and reproductive proliferation in the following growing season but are often more susceptible to freezing than twig tissues (Sakai and Larcher, 1987). Further study in this area is warranted, especially study of the diversity and mechanisms involved in the freezing behaviors of leaf and flower buds. However, because of the complexity of the phenomenon, the development of new methods that can be used to determine changes at the tissue level are necessary.

Conventionally, the freezing behaviors of tissues have been determined using DTA (Quamme, 1995). With DTA alone, it is often difficult to locate the source of exotherms. Excising the plant parts is one way to show the source of exotherms. Excision, however, often introduces artifacts in freezing events and the precise excision of desired tissues is technically difficult. Visual observation of frozen tissues (Ishikawa and Sakai, 1981, 1982, 1985), NMR spectroscopy (Burke et al., 1976; Kaku et al., 1985; Rajashekar, 1989), freeze-fracture electron microscopy (Pearce and Willison, 1985), and scanning electron microscopy of small, frozen tissue specimens (Malone and Ashworth, 1991) have also been used to supplement DTA data. However, none of these methods allows the organized (i.e. systematic) freezing behaviors of various tissues in a single sample to be followed at different temperatures.

In the last two decades there has been considerable progress in high-resolution NMR microimaging, also termed NMR microscopy (Callaghan, 1991; Price, 1998). This technique has been applied to follow changes in the state of water in plants during physiological processes (MacFall and Johnson, 1996; Roberts, 1996) such as dormancy development in some fruit tree buds (Faust et al., 1991; Rowland et al., 1992; Liu et al., 1993), flower bud development, and fruit ripening (Maas and Line, 1995). There has, however, been little application of NMR microscopy to the study of cold-hardiness. Millard et al. (1995) applied it to determine the differences in the properties of water between spring and winter wheat crowns during cold acclimation and freezing, but their study was not intended to clarify complex freezing behaviors in woody plants. Recently, we began NMR-microscopy studies of freezing behaviors in various cold-hardy plants such as azalea (*Rhododendron japonicum*; Price et al., 1997).

* Corresponding author; e-mail isikawam@abr.affrc.go.jp; fax 81–298–38–7408.

Abbreviations: DTA, differential thermal analysis; FOV, field of view; HTE, high-temperature exotherm; LTE, low-temperature exotherm; T_1, spin-lattice relaxation time; T_2, spin-spin relaxation time.

Acer is one of the most common genera of trees in temperate, late-successional forests in Japan and is diverse in its bud structure and growth patterns (Sakai, 1990). The degree of mid-winter cold-hardiness in the species examined is also highly variable, ranging from −25 to −70°C in the leaf buds and twig xylem and from −30 to −70°C in the twig cortex (Sakai, 1982). Flower and leaf buds are often the organs that are most susceptible to freezing, but the reason for this remains unknown (Sakai, 1982; Sakai and Larcher, 1987). *Acer* is an interesting genus with which to study the freezing behavior of leaf and flower buds, but to our knowledge, there have been few previous attempts.

In this study we attempted to determine the freezing behaviors of various tissues in the flower and leaf buds of *Acer japonicum* by using NMR microscopy with high-precision temperature control. From ^{1}H-NMR images of the buds taken at differing subfreezing temperatures, it was possible to visualize the dynamic process of contrasting freezing behaviors in various tissues, including the extraorgan freezing in the primordial inflorescence and shoot. Our results show that NMR microscopy is a powerful, noninvasive tool for locating freezing events and supercooling in complex tissues.

MATERIALS AND METHODS

Terminal leaf and flower buds of full-moon maple (*Acer japonicum* Thunb.) attached to twigs were collected from the Tsukuba Experimental Botanical Garden (Ibaraki, Japan) in December 1996 and February 1997 and stored at 5°C prior to use.

NMR Microscopy

^{1}H-NMR microscopy of *A. japonicum* leaf and flower buds was conducted on an NMR spectrometer (DRX 300, Bruker, Billerica, MA) operating at 300 MHz. A 10-mm ^{1}H-imaging insert was used in the probe for imaging the buds. Cold nitrogen gas was used for cooling. The temperature of the probe head was calibrated using the temperature-dependent chemical shifts of the ^{1}H resonances of methanol (Van Geet, 1968, 1970). Since the electronics in the imaging probe are temperature sensitive, the probe was retuned at each temperature. Images were acquired using leaf and flower buds with about 0.5 cm of the twig attached. The end of the twig was wrapped with a small amount of Parafilm (American National Can, Greenwich, CT) to reduce evaporation during the imaging process. The bud was slid into a 10-mm NMR tube with the twig pointing up, and the tube was capped, placed into a spinner, and pneumatically lowered into the NMR probe in the magnet. The method by which the sample was placed into the imaging probe combined with the natural asymmetry of the buds hindered the accurate positioning of the bud with respect to the axes of the magnetic field gradient coils used in the imaging procedure. Therefore, the images were acquired using a multislice, multiecho pulse sequence to ensure that all relevant parts of the bud were imaged in reasonable time (Fig. 1).

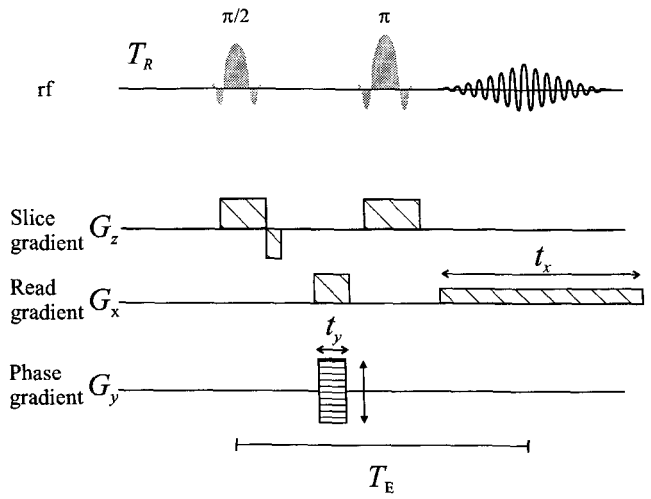

Figure 1. A schematic representation of the multislice, multiecho imaging sequence used in the present work. A slice is first selected using a gradient echo by applying a selective $\pi/2$ radio frequency pulse in the presence of the slice gradient (G_z). The slice is then sampled with two orthogonal gradients (i.e. G_y, the phase gradient; and G_x, the read gradient), producing a Cartesian raster that subdivides the slice into a matrix with (typically) 128 × 128 elements. T_E denotes the echo time, the duration from excitation by the $\pi/2$ pulse to signal acquisition. Since the imaging sequence is based on a spin echo, only those spins with T_2 relaxation times sufficiently long that their signal survives the duration of T_E will contribute to the observable signal. T_R denotes the recycle delay and corresponds to the duration from the end of signal acquisition until the beginning of the next excitation (scan). Typically, T_R is about a second, and T_E is less than 10 ms. If $T_R < 5 \times T_1$, then the image will be T_1-weighted, resulting in a decreased signal intensity due to saturation.

Normally, an FOV of 10 by 10 mm digitized into 128 pixels in each direction (i.e. the in-plane resolution was typically 78 μm) and a slice thickness of 500 μm was used unless otherwise noted. This degree of resolution was deemed to be a suitable compromise between resolution and acquisition time (i.e. the signal-to-noise ratio was proportional to the volume element). Typical image-acquisition parameters were a recycle delay of 1.2 s and an echo time of about 7 ms (the minimum possible echo time given the other acquisition parameters; Fig. 1). Each set of four multislice images required about 20 min to acquire using these experimental parameters. The distance between successive echo planes was 0.5 mm.

The factors that determine the contrast in images inherently contain contributions from T_2 and T_1 of the studied nuclei (protons in the present case). In the present series of experiments we used a long recycle delay and a short echo time, so the contrast in the intensity in the images should predominantly reflect the density of mobile protons (mainly from liquid water). The spin-spin relaxation rate (i.e. $1/T_2$) and consequently the line width of the water resonance increase drastically as the reorientational motion of the water molecule decreases as it becomes ice. In the *A. japonicum* buds studied, the (liquid) water had a sufficiently long T_2 such that its signal remained and was measurable at the end of the echo period in the imaging pulse sequence. However, water in the ice state has a

submillisecond T_2 and consequently is no longer detected at the end of the echo period. In this sense, the echo period served as a mobility filter and allowed the discrimination between water in the liquid and ice states. Therefore, in the images presented, the relaxation times served as the major source of contrast. The light areas contain liquid water and the areas that have become dark represent frozen areas (or very low proton density).

With the image analysis software, the intensity in an image is automatically normalized. To allow direct comparisons of the proton signal intensities (mainly resulting from the unfrozen water) taken at different temperatures, we attempted to display the images in an unnormalized (i.e. absolute intensity) manner. The corrections used are described in detail in "Results and Discussion."

The NMR imaging of *A. japonicum* buds was repeated twice or more, and only one data set is shown here. Similar images were obtained in the other data set. The relative areas of the primordial inflorescence and primordial shoot in the images were determined gravimetrically (i.e. these sections of the images were removed and weighed).

DTA

DTA was performed by cooling excised leaf and flower buds on twigs with a length of about 1 cm at 5°C/h in a programmable deep freezer (model FPR-120S, Fuji Ika Sangyo, Japan). Exothermic events were detected with a copper-constantan thermocouple inserted between the bud scales or in the twig pith and amplified 40 to 100 times prior to recording (Ishikawa and Sakai, 1982). Buds collected in December ($n = 6$) and February ($n = 6$) were separately cooled from 20°C down to −40°C.

Viability of Primordial Shoot and Inflorescence

The viability studies were performed concurrently with the DTA above but in a separate and thermally isolated chamber in the refrigerator used for the DTA; therefore, cogent temperatures for observing bud viability could be inferred from the LTEs observed. To determine the viability of the primordial shoot and inflorescence, buds on twig pieces were cooled at a rate of 5°C/h, and then, at designated temperatures normally 1 to 3°C apart, the buds were removed and warmed to 4°C. The twigs were then water-cultured at 23°C for 3 weeks. At the end of that period the viability of the various tissues was visually determined from the browning of the tissues. The viability at each temperature was determined from 9 to 12 buds. Buds collected in December were used to study viability in the temperature range −15 to −23°C. Similarly, buds collected in February (i.e. more cold-hardy) were used to assess viability between −23 and −28°C.

Visual Observation of Maple Buds

Terminal flower and leaf buds of maple were dissected along the longitudinal axis and observed under a binocular microscope equipped with a photography system at room temperature. The buds were also visually observed at −15°C following slow cooling (5°C/h).

RESULTS AND DISCUSSION

High-Resolution Images of *A. japonicum* Leaf Buds

A ^{1}H-NMR image of an *A. japonicum* terminal leaf bud taken at 1°C with a higher resolution (i.e. pixel size: 39 × 39 μm) than was used in the temperature studies is shown in Figure 2. Various bud tissues visible by optical microscopy (Fig. 3B), such as bud scales and shoot primordia with primordial leaves (Fig. 2), can be seen easily in the NMR image. The bark, xylem, and vascular tissues of the attached twig can also be recognized. The mature pith tissue, which was mostly composed of dead cells, was recognized as a dark region in the NMR image (Fig. 2). This may be a

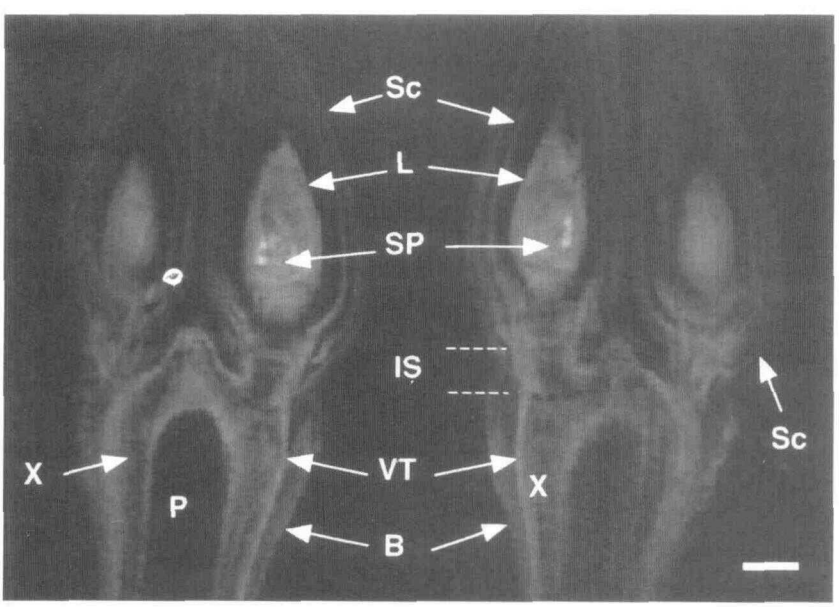

Figure 2. High-resolution longitudinal NMR images taken at 1°C of a pair of terminal leaf buds with 0.5 cm of twig attached from *A. japonicum* collected in December. Shown are two of the four multislice NMR images acquired with an in-plane resolution of 39 μm and a slice thickness of 0.5 mm. The image was scanned 64 times to obtain a good signal-to-noise ratio. Sc, Leaf bud scales; SP, shoot primordium; L, primordial leaf; B, bark; X, xylem; P, pith; IS, immature stem; and VT, vascular tissues. Scale bar represents 1 mm.

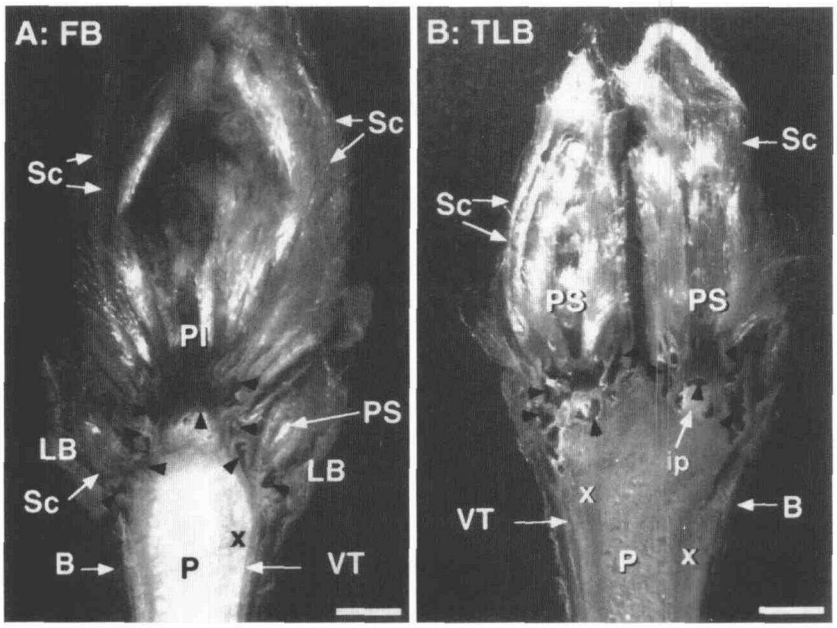

Figure 3. Longitudinal sections of a flower bud (FB; A) and a pair of terminal leaf buds (TLB; B) of *A. japonicum* collected in December and observed under a dissecting optical microscope. Sc, Bud scales; PI, primordial inflorescence; PS, primordial shoot; VT, vascular tissues; B, bark; x, xylem; P, pith; ip, immature pith; and LB, lateral bud. Note the cavity or void (indicated by the black arrowheads) within the bud scales and beneath the primordial inflorescence or primordial shoot. Scale bars represent 1.2 mm.

consequence of low water content and the concomitant formation of air bubbles in the pith tissues, which would result in large magnetic susceptibility differences. Such susceptibility differences would lead to local distortions in the image (Callaghan, 1991).

Primordial shoots and flowers (inflorescences) were attached to the mature stem by an interconnecting immature stem, which comprised bark, vascular tissues, xylem, and pith (Fig. 3). Most of the bud scales were joined to the immature stem, and the innermost scales were attached to the sides of the primordium base (Fig. 3). These immature tissues were also visible in the images (Figs. 2, 4, 5, and 8) and are probably important for extraorgan freezing (which will be discussed later).

Spontaneous Freezing in Bud Scales and Bark Tissues

The intensity of the NMR signals from the bud scales and the bark tissues of both mature and immature stem (Figs. 4 and 5) greatly decreased when the leaf and flower buds of *A. japonicum* were cooled to −7°C. This indicates spontaneous freezing of these tissues, most probably extracellular freezing, which corresponds to the HTE in the DTA profile (Fig. 6). When the buds were further cooled to −14°C, the signal intensity of these tissues further decreased, implying that the tissues had little unfrozen water (Figs. 4 and 5). This is consistent with a previous report (Burke et al., 1974) showing that approximately 65 to 70% of the total tissue water freezes during cooling to −14°C in the extracellular freezing of cold-hardy dogwood bark.

Localization of Ice

Because both frozen tissue and (macroscopic) ice crystals formed in the ice sink appear as dark regions, they cannot be clearly distinguished in the NMR image. Consequently, to investigate the localization of ice sinks, leaf and flower buds were examined visually by dissecting them at −15°C (data not shown). It was found that ice crystals were localized within the basal part of bud scales and beneath the flower or shoot primordium (the upper part of the immature pith). The accumulation of ice in these tissues resulted in the formation of cavities or voids, which were recognized even after thawing (Fig. 3). The location of the ice sinks was similar to that observed in leaf buds of *Acer pseudoplatanus* (Dereuddre, 1979), fir, spruce, and larch (Sakai and Larcher, 1987) and in flower buds of peach (Quamme, 1978; Ashworth et al., 1989). In the flower buds of cold-hardy azalea (Ishikawa and Sakai, 1982) and dogwood (Ishikawa and Sakai, 1985), ice accumulated only in the bud scales.

Deep Supercooling in Xylem Tissues of the Twig

The mature xylem tissues of *A. japonicum* remained unfrozen (showing high signal intensity) even at −21°C (Figs. 4 and 5). This is consistent with the DTA profile of the twig piece, which has a broad LTE starting at approximately −30°C (Fig. 6C). In the xylem of temperate, deciduous trees it is generally believed that only the xylem ray parenchyma exhibit deep supercooling. However, the acquired images looked as if the entire xylem remained unfrozen (Figs. 4 and 5). This is probably because the in-plane resolution of 78 μm was too large to observe ray parenchyma cells (usually 20–30 μm in diameter), and therefore the intensity of each voxel reflects the averaged signal intensity of the xylem parenchyma and other xylem tissues. Therefore, from our data it is not possible to confirm whether only the xylem ray parenchyma supercool. Within the xylem images acquired (Figs. 2, 4, and 5), the innermost layer (corresponding to the primary xylem) and the outermost layer (which is next to the cambium) showed higher intensity than the central part.

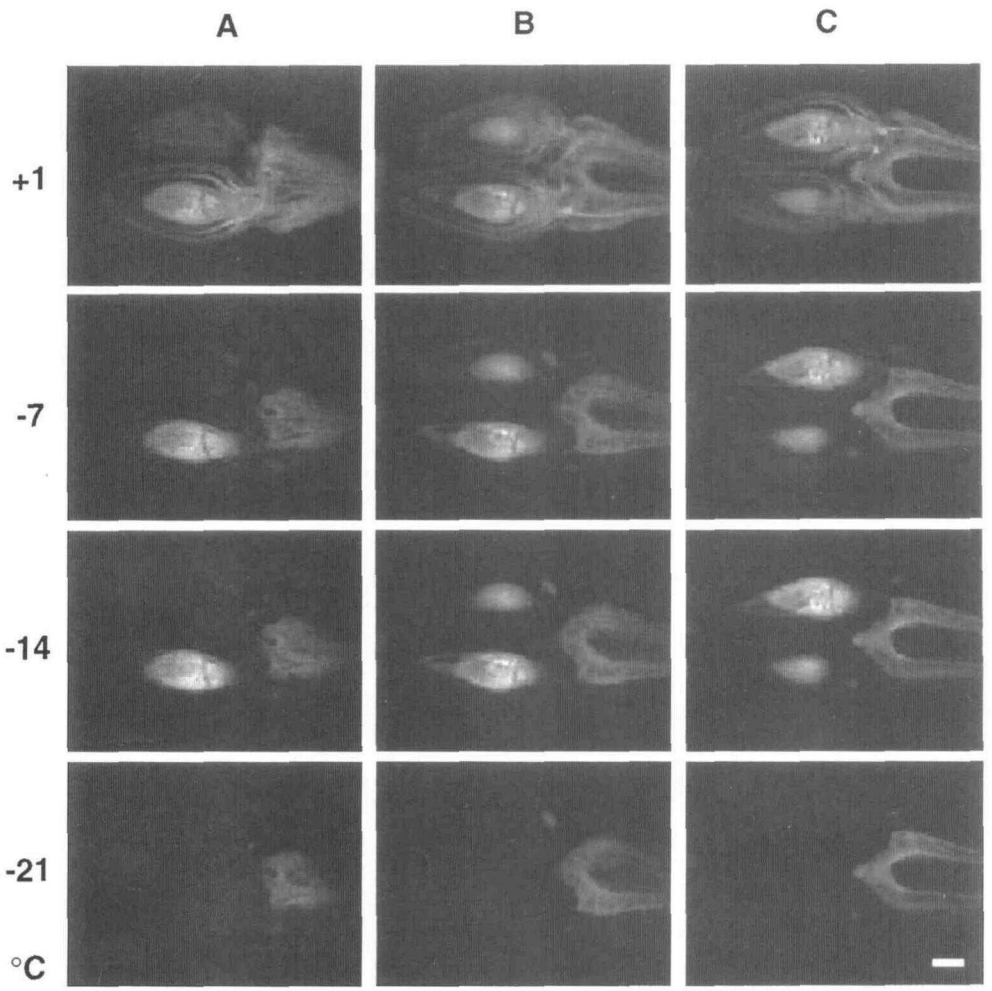

Figure 4. Longitudinal NMR images taken at 1, −7, −14, and −21°C of the same pair of *A. japonicum* terminal leaf buds collected in December. The bud was kept in the imaging probe unmoved during the entire imaging process. The multislice images (four contiguous longitudinal slices were observed at each time) were acquired using 128 × 128 pixels and an FOV of 10 × 10 mm (only the areas showing the sample images are presented). Each image is the average of eight scans. The bud was cooled at 5°C/h and left at the designated temperature for 10 min before the images were acquired. Three (A–C) of the four slices at each temperature are shown to allow the freezing processes in different regions of the bud to be better visualized. Scale bar represents 1 mm.

Supercooling in Shoot and Flower Primordia and the Relationship to Survival

In terminal flower buds of *A. japonicum* collected in December, the primordial inflorescence remained unfrozen (showing high signal intensity) at −14°C but the entire inflorescence froze (i.e. the signal disappeared) at −21°C (Fig. 5). This was consistent with the LTE produced in the range of −19 ± 2°C in December buds when cooled at 5°C/h (Fig. 6A). In terminal leaf buds of *A. japonicum* (December buds), the primordial shoots, including the primordial leaves, remained unfrozen at −14°C but the signal disappeared in the −21°C image (Fig. 4). This was consistent with the LTEs recorded between −18 and −22°C in the DTA profile (Fig. 6B). The LTEs produced by the terminal flower and leaf buds correlated well with the lethal temperature for the flower and shoot primordia. This was shown by rewarming buds that had been cooled in the DTA chamber (at 5°C/h) to different points in the temperature range at which the LTEs occurred (Fig. 6, A and B). Similar close correlation between the LTE range (usually produced between −23 and −28°C) and lethal temperature was found in the terminal flower and leaf buds collected in February (data not shown).

The Boundary between the Frozen and Supercooled Tissues

In both flower and leaf buds, the boundary between the supercooled and frozen tissues was distinctly seen at −7 and −14°C (Figs. 4 and 5). In the image acquired at 1°C, closer observation revealed a darker area between the immature pith and the flower primordium (Figs. 5B and 8), which probably corresponds to the cavity beneath the

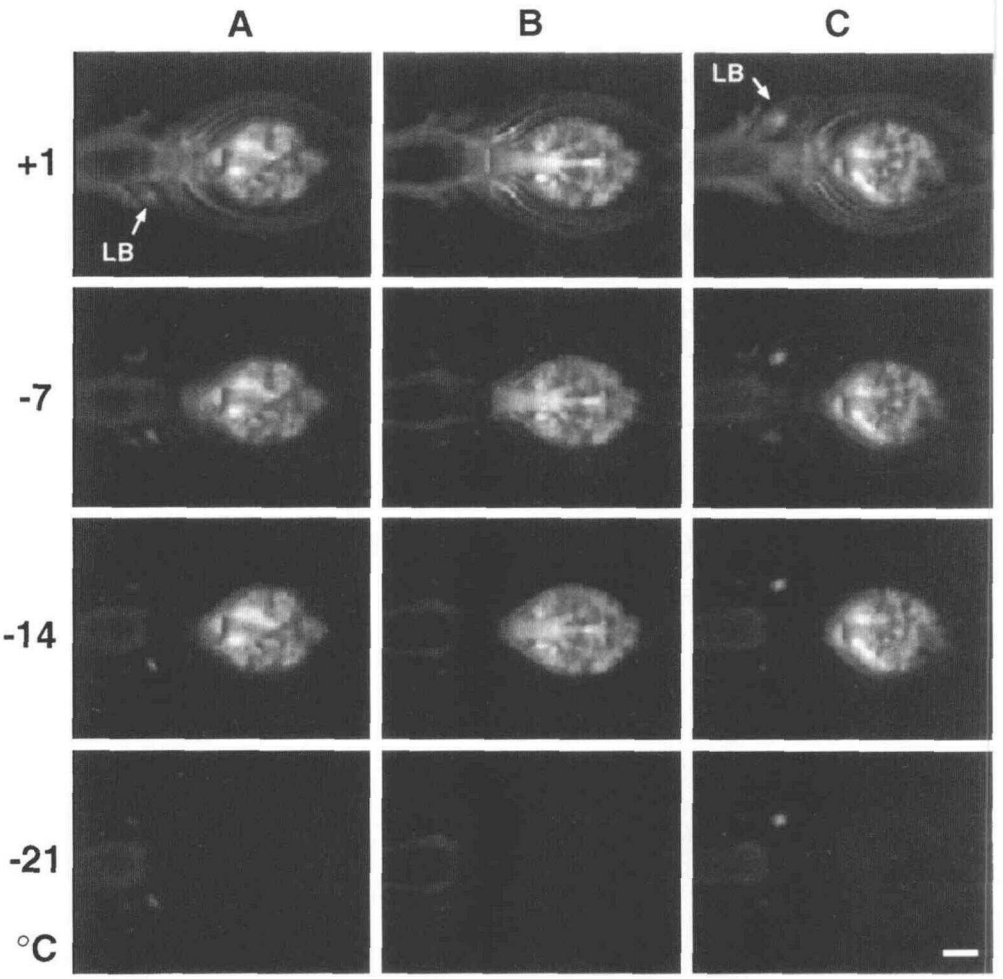

Figure 5. Longitudinal NMR images taken at 1, −7, −14, and −21°C of the same *A. japonicum* flower bud collected in December. The procedure was as in the legend of Figure 4. Only three (A–C) of the four slices acquired at each temperature are shown. LB, Lateral bud. Scale bar represents 1 mm.

flower primordium (Fig. 3). Upon cooling to −7°C, this area became further darkened (probably accommodating ice) and extended outward, forming dark regions in the upper part of the immature xylem (Figs. 5B and 8). This dark region is more clearly recognized when the tissues were imaged in a tangential plane at −7°C (Fig. 5A). It appears that the flower primordium was isolated from other tissues by the dark rectangle perpendicular to the bud axis (this is especially clear in Fig. 8 and is marked by an arrow). During cooling to −14°C, the dark region in the immature xylem extended basipetally, forming a large, dark area in the axis of the bud (Figs. 5 and 8). The formation of a similar dark region in the interconnecting immature stem was also observed in the terminal leaf buds and in the lateral leaf buds (Figs. 4 and 5) but not as distinctly as in the flower bud because of the lower relative resolution. The boundary between the frozen innermost scales and the basal part of the unfrozen primordial inflorescence was also recognized (Fig. 8).

In peach flower buds the formation of a dry region in the bud axis at the initial stage of freezing has been postulated to be important for the supercooling of flower primordia (Quamme, 1978). Using ^{1}H-NMR microimaging, we found that a much larger but gradually darkened area (compared with maple buds) was formed in the axis part of the inflorescence in the flower buds of several species of cold-hardy *Rhododendron* cooled slowly to −7 and −14°C (M. Ishikawa, H. Ide, W.S. Price, and Y. Arata, unpublished data). Whether these dark regions in the NMR images of the bud axis were formed by partial freezing or dehydration (water migration to the adjacent ice accumulation site or "ice sink") remains to be investigated. However, in the maple buds studied, it is tempting to postulate that the darkening area in the immature xylem results from dehydration, because it initiates in the vicinity of the ice sink at the basal part of the scales (Fig. 3) and gradually extends along the basipetal direction (Figs. 5B and 8). Because the supercooled and frozen tissues are in close proximity, the boundary tissues must function as a barrier to ice propagation from the frozen tissues. Whether this barrier is of a structural or biochemical nature remains unknown; however, NMR microscopy can locate the boundary and reveal its behavior in response to subfreezing temperatures by visualizing the unfrozen water.

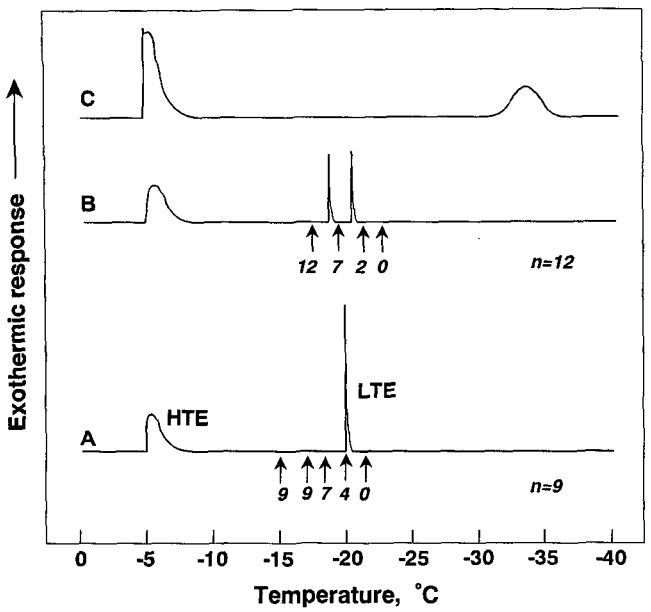

Figure 6. A, Typical DTA profile of an *A. japonicum* flower bud collected in December with 1 cm of twig attached. The bud was cooled at 5°C/h and showed an HTE at −5°C and an LTE in the range of −19 ± 2°C. Typical DTA profiles of a pair of *A. japonicum* terminal leaf buds collected in December having an HTE at −5°C and LTEs between −18 and −22°C (B) and the twig showing an HTE at −5°C and a broad LTE from the xylem starting at approximately −30°C (C). To emphasize the correlation between viability and the production of LTEs, the number of viable buds in the viability study removed at the indicated temperatures are shown in italics beneath the DTA profiles (A and B). In the viability study 9 flower buds and 12 terminal leaf buds were used at each temperature.

Reduction in the Sizes of Shoot and Flower Primordia during Slow Cooling

When the buds were cooled from −7 to −14°C, a gradual decrease (with both acropetal and centripetal gradients) in the signal intensity was noticed mainly in the basal part of these tissues adjacent to the ice sinks (Figs. 4, 5, and 8) within the supercooled primordial inflorescence and primordial shoots. Cooling of the buds to −7°C and then to −14°C also affected the total size of supercooled inflorescence and shoots (Figs. 4, 5, and 8). The percentage areas of the unfrozen primordial tissues as determined from NMR microscopy is shown in Figure 7. There were approximately 10% decreases in the area of the images of both primordial inflorescence and primordial shoots upon cooling from +1 to −14°C.

A closer view of the NMR images (Fig. 8) revealed a shrinkage of the peduncle in the inflorescence along the long axis. The gravimetrically determined values may have underestimated the size reduction, because we measured only the whole whitish silhouette in the image, and the silhouette included air spaces (which appear as dark regions) between the highly reticulated structures in the primordial flower and shoot. These observations imply that the water in the supercooled primordial shoots and flowers moves to the ice sink through the basal part of the primordia during slow cooling (Fig. 8).

Similar slow dehydration of supercooled organs was observed in flower buds from several species of cold-hardy azalea (Ishikawa and Sakai, 1982), conifer leaf buds (Sakai and Larcher, 1987), and *Prunus* (Rajashekar and Burke, 1978). Ishikawa and Sakai (1982) measured the water content of florets dissected under subfreezing temperatures during slow cooling at 5°C/d to −15°C. The slow dehydration of the supercooled organ resulted in an enhancement of the supercooling of the organ and complementary ice accumulation in the ice sink at naturally occurring cooling rates (Ishikawa and Sakai, 1982). NMR microscopy successfully visualized a similar complex freezing event (i.e. extraorgan freezing) in terminal leaf and flower buds of *A. japonicum* except for the accumulation and localization of ice. This is one of the few cases (other examples include blueberry and the genera *Cornus* and *Forsythia*) in which extraorgan freezing has been shown in buds other than those of conifers and the genera *Rhododendron* and *Prunus* (Quamme, 1995).

Maximum cold-hardiness (the lowest survival temperature with no symptom of injury) reported for terminal leaf buds of *A. japonicum* is −30°C (Sakai, 1982). This value is lower than the LTE (−23 to −28°C) measured with February buds but can be accounted for by cold-hardening (−3°C for 14 d and −5°C for 3 d) and slower cooling rates (2.5°C/h) used for cold-hardiness determination. The slower cooling enables more extensive dehydration of the supercooled primordia, which results in lowering the LTE. However, the cold-hardiness data (Sakai, 1982) and the rate of size reduction (Fig. 7) imply that the water removal rate is not great enough to remove all of the freezable water from the supercooled primordia. Therefore, there is a survival limit higher than the homogeneous nucleation temperature of pure water (approximately −40°C; Angell,

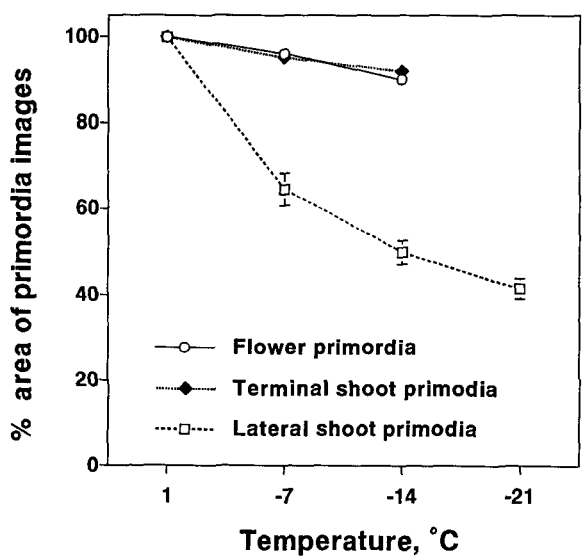

Figure 7. Changes in the relative areas of the primordial inflorescence and the primordial shoot (both terminal and lateral) from the NMR images of *A. japonicum* buds cooled to subfreezing temperatures at 5°C/h. The data presented are the means ± SE of three to six tissues (only SEs greater than 1% are shown).

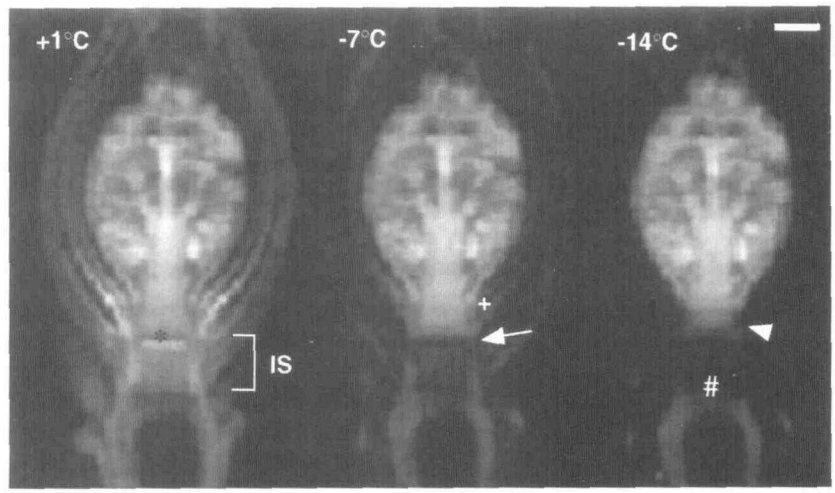

Figure 8. A higher magnification view of the primordial inflorescence imaged in Figure 5B. In the image acquired at 1°C, a darker area between the pith and flower primordium was seen (*), which probably corresponds to the cavity beneath the flower primordium (Fig. 3). The formation of dark regions in the upper part of the immature xylem (indicated by the arrow) at −7°C and its spread to the basipetal direction (#) at −14°C are visible. By comparing the −7 and −14°C images, we also noticed a gradual decrease in the signal intensity of the basal part of the inflorescence (acropetally from the bottom and also centripetally from the sides; indicated by the arrowhead) and a shrinkage of the peduncle along the long axis. These observations imply water withdrawal from the supercooled inflorescence to the ice sinks located beneath the primordium (*) and in the innermost scales beside the basal part of the primordium (+). IS, Immature stem. Scale bar represents 1 mm.

1982). This type of extraorgan freezing has been classified as type III and can be seen in various cold-hardy azalea species (Ishikawa and Sakai, 1982).

Freezing Behavior of Lateral Leaf Buds

In the lateral buds at the base of terminal flower buds, the shoot primordia remained unfrozen even at −21°C, as shown in the NMR images (Fig. 5). The size of the supercooled lateral shoot primordia in the images was reduced by 58% during cooling from +1 to −21°C, and the rate was much greater than in terminal flower or shoot primordia (Fig. 7). If the buds were cooled further with this rate of size reduction, the shoot primordia would lose a significant proportion of the tissue water. In fact, DTA of terminal flower buds with lateral buds detected no LTE between −21 and −40°C (cooling rate 5°C/h; Fig. 6A). Visual determination of the viability of the same buds (cooled to −40°C) revealed that the lateral shoot primordia were all viable (the flower primordia were killed). The lateral buds of *A. japonicum* have been reported to consistently tolerate −70°C after full cold-hardening (Sakai, 1982).

These facts imply that lateral shoot primordia of *A. japonicum* undergo type I extraorgan freezing (Ishikawa and Sakai, 1982), in which the organ is dehydrated at a considerable rate during slow cooling and can tolerate the resultant fully dehydrated state. Since all of the freezable water in the organ is removed during slow cooling, the organ can tolerate temperatures lower than the homogeneous ice nucleation temperature (approximately −40°C) and sometimes even submersion in liquid nitrogen. Type I extraorgan freezing has been observed in leaf buds of very cold-hardy spruce and larch and in hydrated seeds of small size (Ishikawa and Sakai, 1982; Sakai and Larcher, 1987).

Technical Problems

The terminal flower bud samples used in this study were nearly symmetrical and it was experimentally easy to obtain images of longitudinal sections at the desired position. However, for the more asymmetrical terminal vegetative bud samples it was much more difficult to align the buds with respect to the axes of the imaging gradients so that the orientation of the slice selection in the imaging sequence corresponded to the axis in the flower bud. To alleviate this difficulty we used a multislice, multiecho imaging sequence in which four different slices were acquired concurrently. In theory, a full three-dimensional imaging data set could be acquired and arbitrary orientations could be reconstructed from the data set. However, the time required to acquire such a data set is intolerably long for our experimental purposes.

When the images of a bud taken at different temperatures are compared, it is important to consider what factors modulate the signal intensity apart from that resulting directly from the water to ice transition and to adjust the image intensities if necessary. The sensitivity of the NMR experiment increases as the temperature decreases, since the population difference between nuclear energy levels (which are the origin of the NMR signal) increases. This difference is described by the Boltzmann distribution (Goldman, 1992). Therefore, the integrated signal intensity increases by approximately a modest 10% on going from 1°C down to −21°C (the effect was nearly imperceptible in the images). Furthermore, there is a slight increase in probe sensitivity due to the decrease in Johnson noise in the radio frequency coils as they are cooled. However, these increases are largely offset by the gradual decrease in the water T_2 while it is in the liquid state (i.e. the transition to

fthe ice state is marked by a catastrophic decrease). The water is in a number of different environments in the leaf bud, so no single relaxation time describes all of the liquid water present in the leaf bud. Therefore, because of the canceling nature of the above effects and the heterogeneous environments of the liquid water, corrections were not made to the image intensity (apart from ensuring that the images were scaled to the same factor in the Fourier transformation step in the image reconstruction and in the display of reconstructed image).

In separate experiments we checked the effect of temperature decreases on the signal intensity in the NMR images using pure water, potato stem (a non-cold-hardy material), and wintering maple stem (a cold-hardy material) placed together in a 5-mm tube (Price et al., 1998). The results showed that there were significant increases in the images of the pure water and potato stem caused by the decrease in temperature from 23 to −18°C. The pure water at 23°C has a much longer T_1 than the recycle delay (1.2 s), and the intensity of the water image is considerably attenuated because of the effects of T_1 saturation. However, with decreasing temperature, the water T_1 decreases, which allows more complete relaxation of the water between scans and, subsequently, a higher signal intensity. The same effect, but to a lesser extent, occurred in the potato stem. In contrast, there was an almost negligible increase in the signal intensity of the maple xylem. This is because the water in the maple xylem is in a viscous medium that results in a long reorientational correlation time for the water molecule; consequently, the water has a sufficiently short relaxation time even at room temperature and the T_1-saturation effects were minimal. The results of the maple stem study also showed that the overall effect of the decrease in temperature (signal-to-noise ratio improvement and Boltzmann distribution, etc.) on the signal intensity was small, as was predicted in the preceding paragraph. As shown in Figures 4 and 5, the signal intensity of the primordial inflorescence and shoots increased slightly with decreasing temperature, but this is mainly due to the effect of T_1 saturation. Water in differing environments showed different responses to temperature decreases in the NMR images, but these changes in signal intensity were small with respect to the changes caused by freezing events and in no way affect the interpretation of the images (Figs. 4 and 5).

Because the FOV is smaller than the sample dimensions, there is some ghosting (i.e. highly attenuated reflection) from sample outside the FOV. However, the only total solution is to use an FOV larger than the sample, with a corresponding loss in resolution, assuming that the image is acquired with the same number of pixels. Thus, we have used an FOV smaller than the sample size, because the ghosting is not very significant and did not hinder the interpretation of the images (Fig. 5).

Advantages of NMR Microscopy for the Study of Freezing Behaviors

Apart from the unique, noninvasive nature of NMR imaging, which allows the study of ongoing physiological processes in live samples, the other enormous advantage of NMR imaging is its sensitivity to a wide range of chemical (i.e. chemical shift; Pope et al., 1993; Ishida et al., 1996) and physical contrast mechanisms such as diffusion, flow, and relaxation (Kockenberger et al., 1997). These contrast mechanisms are observable by other methods. In the present experiments the contrast in the images was provided by the change in the water relaxation times resulting from the decrease in motion of water molecules as they enter the ice state. As noted above, the water in different parts of the leaf buds has different characteristics (e.g. different T_1s and T_2s, etc.), and when different imaging sequences and appropriate parameters are used, these differences can be used to provide additional sources of contrast (data not shown). Thus, the imaging technique and parameters can be "tuned" to be sensitive to the different states of water in leaf buds, and the resulting information is ultimately useful in helping to understand the mechanisms involved in freezing behaviors and cold acclimation. At present we are investigating the application of more sophisticated NMR-imaging techniques involving motional contrast factors (Price, 1998) in an attempt to separate dehydration from ice formation in plant tissues.

Recently, IR thermography has been effectively used to study ice nucleation and propagation in intact plants (Wisniewski et al., 1997). This method noninvasively images the latent heat flow released from the surface of tissues being frozen and can detect rapid phenomena. In contrast, with NMR microscopy it is more difficult to detect such rapid phenomena while maintaining high levels of resolution. However, it can noninvasively detect fine spatial distribution of unfrozen water inside the complex tissues, as was shown in this study.

CONCLUSIONS

Our results clearly show that NMR microscopy is a useful tool for studying freezing behaviors in plant tissues. Basically, a ^{1}H-density image taken at a subfreezing temperature reveals the fine localization of unfrozen water in the sample. By comparing NMR images taken at various subfreezing temperatures, we could visualize contrasting freezing behaviors in various tissues of *A. japonicum* (e.g. extracellular freezing in the bark and bud scales and deep supercooling in the xylem). In the flower and shoot primordia, the dynamic processes of extraorgan freezing were imaged. The formation of a possible barrier against ice propagation and subsequent gradual dehydration through the basal part of the supercooled organ were seen. Extraorgan freezing of various types may be more widespread in leaf and flower buds of temperate woody species, as was exemplified here in *A. japonicum*.

NMR microscopy noninvasively provides visual information on tissue-specific and tissue-tissue interactions. We hope that, in combination with other methods, it will help to promote an understanding of the complex mechanisms and diversity involved in freezing behaviors. Examples are identifying the barrier against ice propagation from already frozen tissues into the supercooled tissues in extraorgan freezing (Ishikawa and Sakai, 1985; Quamme, 1995),

elucidating the relationship of freezing behaviors to bud morphology (Rajashekar and Burke, 1978; Warmund et al., 1991; Kader and Proebsting, 1992) and/or phylogeny (Ishikawa and Sakai, 1982), and determining exotherms from tissues not otherwise identifiable. We are in the process of performing a series of studies on these issues using NMR microscopy.

ACKNOWLEDGMENTS

We thank Dr. Shunji Nakagawara (Suntory Ltd., Osaka, Japan) for his interest in this work and Ms. Tomomi Kitashima for her technical assistance.

Received July 21, 1997; accepted September 12, 1997.

LITERATURE CITED

Angell CA (1982) Supercooled water. *In* F Franks, ed, Water and Aqueous Solutions at Subzero Temperatures. Plenum Press, New York, pp 1–81

Ashworth EN, Davis GA, Wisniewski ME (1989) The formation and distribution of ice within dormant and deacclimated peach flower buds. Plant Cell Environ **12:** 521–528

Becwar MR, Rajashekar C, Hansen Bristow KJ, Burke MJ (1981) Deep undercooling of tissue water and winter hardiness limitations in timberline flora. Plant Physiol **68:** 111–114

Burke MJ, Bryant RG, Weiser CJ (1974) Nuclear magnetic resonance of water in cold acclimating red osier dogwood stem. Plant Physiol **54:** 392–398

Burke MJ, Gusta LV, Quamme HA, Weiser CJ, Li PH (1976) Freezing and injury in plants. Annu Rev Plant Physiol **27:** 507–528

Callaghan PT (1991) Principles of Nuclear Magnetic Resonance Microscopy. Oxford University Press, Oxford, UK

Dereuddre J (1979) Etude comparative du comportement des bourgeons d'arbres en vie ralentie, pendant un refroidissenment graduel des rameaux. Bull Soc Bot Fr **126,** Lettres bot: 399–412

Faust M, Liu D, Millard MM, Stutte GW (1991) Bound versus free water in dormant apple buds-a theory for endodormancy. Hortscience **26:** 887–890

George MF, Burke MJ, Pellet HM, Johnson AG (1974) Low temperature exotherms and woody plant distribution. Hortscience **9:** 519–522

Goldman M (1992) Quantum Description of High-Resolution NMR in Liquids. Oxford University Press, Oxford, UK

Ishida N, Koizumi M, Kano H (1996) Location of sugars in barley seeds during germination by NMR microscopy. Plant Cell Environ **19:** 1415–1422

Ishikawa M, Sakai A (1981) Freezing avoidance mechanisms by supercooling in some *Rhododendron* flower buds with reference to water relations. Plant Cell Physiol **22:** 953–967

Ishikawa M, Sakai A (1982) Characteristics of freezing avoidance in comparison with freezing avoidance: a demonstration of extra-organ freezing. *In* PH Li, A Sakai, eds, Plant Cold Hardiness and Freezing Stress, Vol 2. Academic Press, London, pp 325–340

Ishikawa M, Sakai A (1985) Extraorgan freezing in wintering flower buds of *Cornus officinalis*. Sieb. et Zucc. Plant Cell Environ **8:** 333–338

Kader SA, Proebsting EL (1992) Freezing behavior of *Prunus*, subgenus *Padus*, flower buds. J Am Soc Hortic Sci **117:** 955–960

Kaku S, Iwaya M (1979) Deep supercooling in xylems and ecological distribution in the genera *Ilex*, *Viburnum* and *Quercus* in Japan. Oikos **33:** 402–411

Kaku S, Iwaya-Inoue M, Gusta LV (1985) Estimation of the freezing injury in flower buds of evergreen azaleas by water proton NMR relaxation times. Plant Cell Physiol **26:** 1019–1026

Kockenberger W, Pope JM, Xia Y, Jeffrey KR, Komor E, Callaghan PT (1997) A non-invasive measurement of phloem and xylem water flow in castor bean seedlings by nuclear magnetic resonance microimaging. Planta **201:** 53–63

Liu D, Faust M, Millard MM, Line MJ, Stutte GW (1993) States of water in summer-dormant apple buds determined by proton magnetic resonance imaging. J Am Soc Hortic Sci **118:** 632–637

Maas JL, Line MJ (1995) Nuclear magnetic resonance microimaging of strawberry flower buds and fruit. Hortscience **30:** 1090–1096

MacFall JS, Johnson GA (1996) Plants, seeds, roots and soils as applications of magnetic resonance microscopy. *In* DM Grant, RK Harris, eds, Encyclopedia of Nuclear Magnetic Resonance. Wiley, New York, pp 3633–3640

Malone SR, Ashworth EN (1991) Freezing stress response in woody tissues observed using low temperature scanning electron microscopy and freeze substitution techniques. Plant Physiol **95:** 871–881

Millard MM, Veisz OB, Krizek DT, Line M (1995) Magnetic resonance imaging (MRI) of water during cold acclimation and freezing in winter wheat. Plant Cell Environ **18:** 535–544

Pearce RS, Willison JHM (1985) Wheat tissues freeze-etched during exposure to extracellular freezing: distribution of ice. Planta **163:** 295–303

Pope JM, Jonas D, Walker RR (1993) Applications of NMR microimaging to the study of water, lipid, and carbohydrate distribution in grape berries. Protoplasma **173:** 177–186

Price WS (1998) NMR imaging. *In* GA Webb, ed, Annual Reports on NMR Spectroscopy. Academic, London (in press)

Price WS, Ide H, Arata Y, Ishikawa M (1997) Visualization of freezing behaviours in flower bud tissues of cold hardy *Rhododendron japonicum* by nuclear magnetic resonance microimaging. Aust J Plant Physiol **24:** 599–605

Price WS, Ide H, Ishikawa M, Arata Y (1998) Intensity changes in ^{1}H-NMR micro-images of plant materials exposed to subfreezing temperatures. Bioimages (in press)

Quamme HA (1978) Mechanism of supercooling in overwintering peach flower buds. J Am Soc Hortic Sci **103:** 57–61

Quamme HA (1995) Deep supercooling in buds of woody plants. *In* RE Lee, GJ Warren, LV Gusta, eds, Biological Ice Nucleation and Its Applications. APS Press, St. Paul, MN, pp 183–200

Rajashekar C, Burke, MJ (1978) The occurrence of deep undercooling in the genera *Pyrus*, *Prunus* and *Rosa*: a preliminary report, *In* PH Li, A Sakai, eds, Plant Cold Hardiness and Freezing Stress. Academic Press, New York, pp 213–225

Rajashekar CB (1989) Supercooling characteristics of isolated peach flower bud primordia. Plant Physiol **89:** 1031–1034

Roberts JKM (1996) Plant physiology, *In* DM Grant, RK Harris, eds, Encyclopedia of Nuclear Magnetic Resonance. Wiley, New York, pp 3627–3633

Rowland LJ, Liu D, Millard MM, Line MJ (1992) Magnetic resonance imaging of water in flower buds of blueberry. Hortscience **27:** 339–341

Sakai A (1982) Freezing resistance of ornamental trees and shrubs. J Am Soc Hortic Sci **107:** 572–581

Sakai A, Larcher W (1987) Frost Survival of Plants. Responses and Adaptation to Freezing Stress, Ecological Studies 62. Springer-Verlag, Berlin

Sakai S (1990) The relationship between bud scale morphology and indeterminate and determinate growth patterns in *Acer* (Aceraceae). Can J Bot **68:** 144–148

Van Geet AL (1968) Calibration of the methanol and glycol nuclear magnetic resonance thermometers with a static thermistor probe. Anal Chem **40:** 2227–2229

Van Geet AL (1970) Calibration of methanol nuclear magnetic resonance thermometer at low temperature. Anal Chem **42:** 679–680

Warmund M, George M, Takeda F (1991) Supercooling in floral buds of 'Danka' black and 'Red Lake' red currants. J Am Soc Hortic Sci **116:** 1030–1034

Wisniewski M, Lindow SE, Ashworth EN (1997) Observations of ice nucleation and propagation in plants using infrared video thermography. Plant Physiol **113:** 327–334